

A05 Using Seismic Facies Maps in Geological Models

F. CUNHA¹, P. NEFF², O. VOUTAY²

¹Sonangol EP/DEX

Edificio DH – Av. 4 Fevereiro

P.O Box 1316

Luanda - Angola

²Beicip-Franlab

Introduction

Well data alone cannot accurately recover the requested property variations, because of their sparse lateral distribution and their large spacing, compared to the size of the lateral heterogeneities to be modeled. On the opposite and despite its poor vertical resolution, seismic data provide valuable information to overcome such a limitation as it benefits from the highest lateral density of information. Accurate descriptions of the lateral variation of reservoir heterogeneities is a critical issue when generating reservoir models dedicated to history matching and sub-sequent production forecasts.

This paper describes one of the workflow that has been successfully applied on a turbidite field in Angola, which allows (1) extracting reliable constraints from post-stack seismic amplitudes and (2) incorporating them into high-resolution geological models.

Relevant constraints are generated using seismic reservoir characterization techniques, based on seismic inversion followed by seismic facies analysis and generation of net-to-gross maps. Then, for geological modeling, we chose a pluri-gaussian modeling technique, which provides the requested level of flexibility for mixing the obtained map with well data and thus solving the downscaling issues.

Case study

The example used for illustrating the modeling workflow described in this paper is a turbidite field, offshore Angola. The data set used is the following:

- 3D post-stack seismic volume (Figure 1);
- 8 wells with a full set of logs, including sonic, density, gamma ray, resistivity and neutron porosity. A typical well is displayed on Figure 1.
- The reservoir top and bottom in both time and depth.

Extracting the relevant seismic constraints

The seismic reservoir characterization work starts with a model-based multi-channel inversion, calibrated at all wells and that takes into account the stratigraphy within the reservoir interval. Seismic attributes used for reservoir characterization are relative P-impedance traces extracted from the inversion result at the reservoir level.

Because of the heterogeneity of the reservoir under study, no reliable quantitative relationship can be built between seismic attributes and reservoir properties at wells. Consequently, a seismic facies analysis is performed to obtain a reservoir zonation map. This map is then converted into sand proportion map by calibrating the seismic facies against well data.

The technique we use is a non-supervised statistical pattern recognition technique, based on the analysis of the multivariate probability density function of the seismic attributes. This analysis allows identifying the number of natural clusters in the data, each mode corresponding to a specific shape of the traces. The most typical traces of each mode are extracted and then used in discriminant analysis. Two maps are finally obtained: a facies map and a probability map that gives information on the confidence in the classification.

On our example, the final non-supervised seismic facies map exhibits 4 different seismic facies (figure 2). All of them have been recognized by at least one well, and can therefore be interpreted:

- The yellow facies corresponds to zones with the highest proportion of sands with good to very good reservoir properties. The average net-to-gross within this seismic facies has been estimated to 50%.
- The orange facies corresponds to a net-to-gross of 35%, with rather good quality reservoir sands;
- The light blue seismic facies, with intermediate reservoir quality and a net-to-gross of 25%
- The dark blue facies, which corresponds to a non-reservoir facies, with a net-to-gross of less than 2%.

A facies proportion map is derived from this a posteriori interpretation by assigning the relevant net-to-gross calculated at wells to each seismic trace having a probability cut off greater than 80% (Figure 3). This final map, with gaps (in grey on Figure 3) is used as an input in the next high-resolution geological modeling step.

Geological modeling

The Pluri-Gaussian Simulation technique we have selected starts with the analysis of the facies proportions, based on well data and within each reservoir zone. On a practical point of view, one vertical proportion curve is associated to each seismic facies. Based on the vertical proportion curves, a mapping of vertical facies proportions, also called proportion matrix, is generated in such a way that it honours both local facies proportion curves and the facies proportions estimated from seismic data (Figure 4).

Pluri-gaussian modelling requires two variogram models which are used to simulate two gaussian functions. Facies are then defined using thresholds on these two functions. Obviously, the thresholds to be used depend (1) on the relationship between the different facies and (2) on the facies proportions. The facies ordering within the reservoir sequence has been selected to honor the geological model where reservoir sands and shaly sands deposits belong to organized sequences embedded with shales. Figure 5 summarizes the pattern that has been selected for modeling the facies distribution. The same way, the variogram models selected for pluri-gaussian simulations strongly depend on the stratigraphic model and the geometry of deposits that are expected. In this case study, two exponential models have been selected:

- The first one controls the deposits of reservoir facies (sand and shaly sand). It has been selected isotropic.
- The second one controls the distribution of the reservoir (sand + shaly sand) amongst the shales (most present facies). It has been selected anisotropic to recover the main elongation and direction of the reservoir deposits.

As a result, the pluri-gaussian simulation delivers a high-resolution geological model conditioned at wells and honoring the lateral facies variations analyzed on the seismic (Figure 6). This can be easily verified from the obtained model by calculating a net-to-gross map over the reservoir interval. Figure 7 displays the final results and compares both maps to demonstrate the efficiency of the seismic control over the geological model. For further visualizing the impact of seismic reservoir characterization on the obtained geological model, Figure 7 displays a model generated using the same data set (wells, correlation scheme, structural model, etc.), except seismic facies and net-to-gross maps. On this figure, the amount of reservoir facies is the same as before, but their distribution is not constrained laterally. This obviously will have a significant impact on the petrophysical models, after porosity and permeability attribution, thus on the result of the up-scaling, and finally on the dynamic behavior of the model.

Conclusion

The methodology described in this paper for integrating seismic data into high-resolution geological models offer an unmatched flexibility since qualitative (seismic facies maps) and/or quantitative (property maps) geological constraints can be used. The selection of the type of constraint to be generated depends mainly on:

- The quality of seismic data (in terms of signal content and resolution);
- The expected seismic response of the reservoir interval, which depends at the same time on lithology, porosity, fluid content, bed thickness, etc.;
- The relationships that can be detected between seismic attributes and reservoir properties.

At the same time, pluri-gaussian modeling techniques provide very efficient ways of mixing together information derived from seismic and from wells and taking into account the actual reservoir geology.

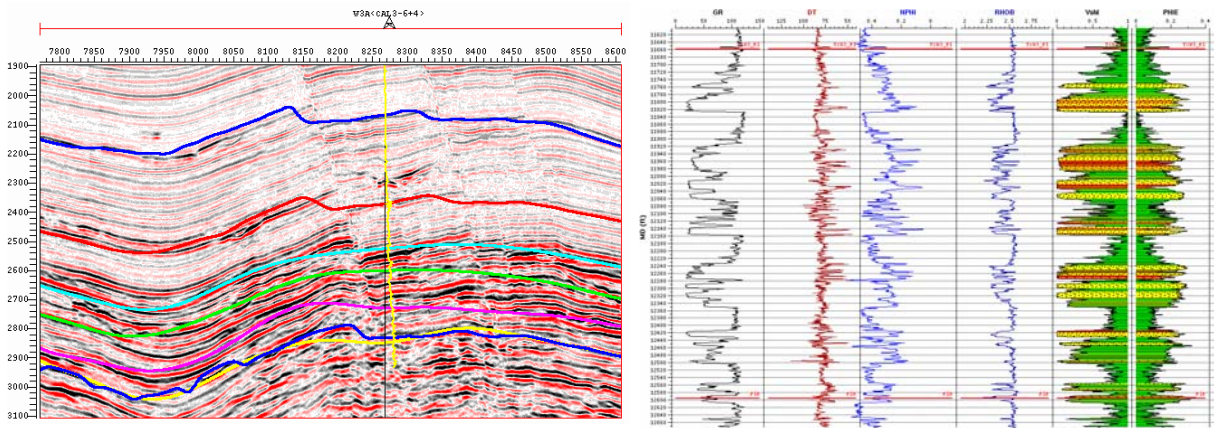


Figure 1: Seismic line and Typical well data

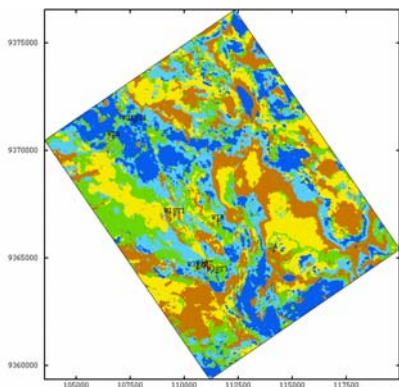


Figure 2: Obtained seismic facies map

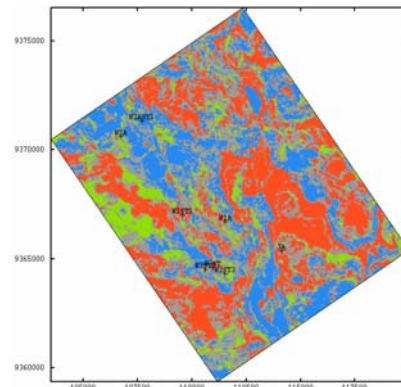


Figure 3: Net-to-Gross map

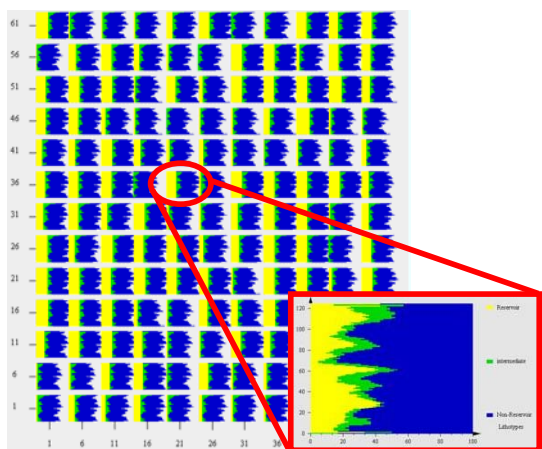


Figure 4: Proportion matrix

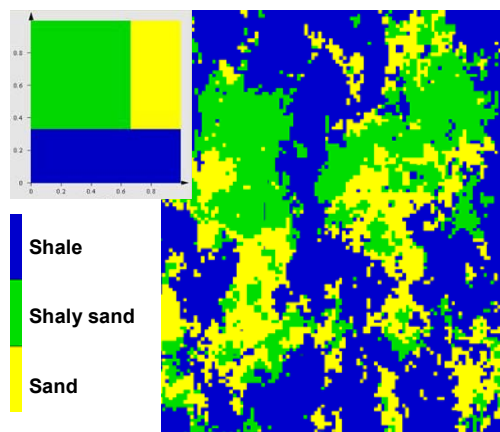


Figure 5: Facies pattern definition and horizon slice

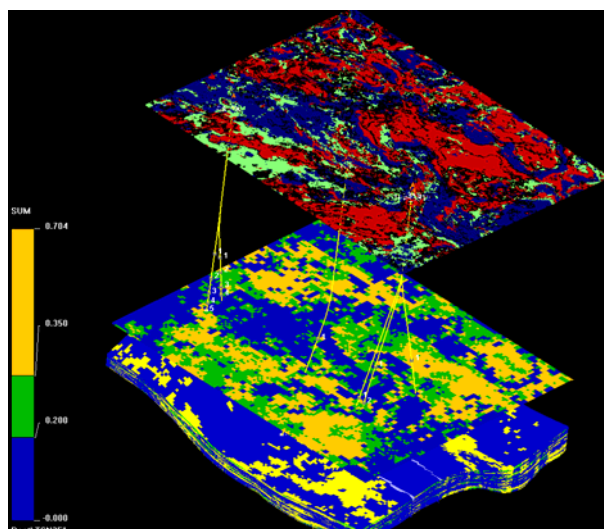


Figure 6: Final model & comparison between input and calculated net-to-gross maps

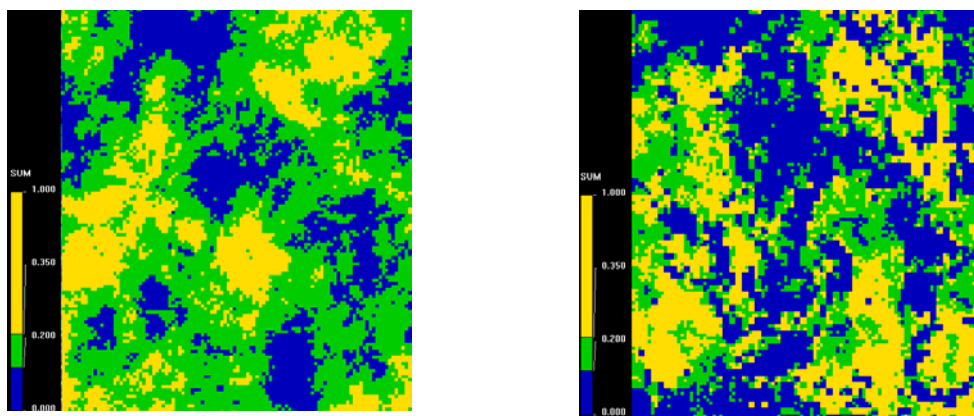


Figure 7: Comparison of calculated net-to-gross maps, without (right) and with (left) seismic constraint